

Catalytic Formation of Hydrogen Peroxide from Coenzyme NADH and Dioxygen with a Water-Soluble Iridium Complex and a Ubiquinone Coenzyme Analogue

Tomoyoshi Suenobu,^{*,†} Satoshi Shibata,[†] and Shunichi Fukuzumi^{*,†,‡,§}

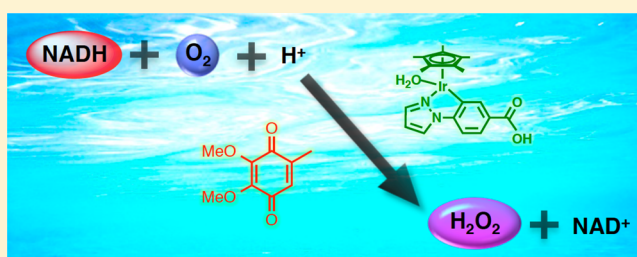
[†]Department of Material and Life Science, Graduate School of Engineering, Osaka University, ALCA and SENTAN, Japan Science and Technology, Suita, Osaka 565-0871, Japan

[‡]Department of Chemistry and Nano Science, Ewha Womans University, Seoul 120-750, Korea

[§]Faculty of Science and Engineering, Meijo University, ALCA and SENTAN, Japan Science and Technology Agency, Nagoya, Aichi 468-0073, Japan

S Supporting Information

ABSTRACT: A ubiquinone coenzyme analogue (Q_0 : 2,3-dimethoxy-5-methyl-1,4-benzoquinone) was reduced by coenzyme NADH to yield the corresponding reduced form of Q_0 (Q_0H_2) in the presence of a catalytic amount of a [C,N] cyclometalated organoiridium complex (**1**: $[\text{Ir}^{\text{III}}(\text{Cp}^*)(4\text{-}(1\text{H-pyrazol-1-yl-}\kappa\text{N}^2)\text{benzoic acid-}\kappa\text{C}^3)(\text{H}_2\text{O})_2]\text{SO}_4$) in water at ambient temperature as observed in the respiratory chain complex I (Complex I). In the catalytic cycle, the reduction of **1** by NADH produces the corresponding iridium hydride complex that in turn reduces Q_0 to produce Q_0H_2 . Q_0H_2 reduced dioxygen to yield hydrogen peroxide (H_2O_2) under slightly basic conditions. Catalytic generation of H_2O_2 was made possible in the reaction of O_2 with NADH as the functional expression of NADH oxidase in white blood cells utilizing the redox cycle of Q_0 as well as **1** for the first time in a nonenzymatic homogeneous reaction system.

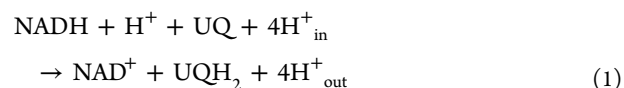


INTRODUCTION

NADH-coenzyme Q oxidoreductase so-called respiratory chain “Complex I” at inner mitochondria membrane of eukaryotes as well as cell membrane of bacteria (prokaryotes) accepts electrons from 1,4-dihyronicotinamide adenine dinucleotide (NADH) and passes electrons to ubiquinone coenzyme Q (UQ) to generate ubiquinol (UQH_2).^{1,2} UQH_2 is known to carry the electrons to the next complex (Complex III, cytochrome bc_1 complex) through the supercomplex formation between Complex I and Complex III.³ UQH_2 is also transported from Complex II (succinate-coenzyme Q reductase) that catalyzes the oxidation of succinate to fumarate with the reduction of UQ to UQH_2 .^{4,5} Inside the mitochondria membrane, UQH_2 exists together with UQ in so-called ubiquinone pool (Q-pool) being relatively mobile.⁶ UQ is also synthesized in the endoplasmic reticulum and Golgi membrane system. In these nonmitochondrial membranes, UQH_2 functions as an antioxidant, which is essential for the defensive system against oxidative stress in tissues.⁷ Actually, UQ was found to be an effective antioxidant for the medical treatment of neurodegenerative diseases.⁸ In this context, mechanistic insight into oxidation of UQH_2 and its analogues with molecular oxygen has been studied with respect to autoxidation.⁹ However, the antioxidant effect of UQ on autoxidation of UQH_2 has yet to be revealed in a homogeneous reaction system, where reaction kinetics can be analyzed with

use of various spectroscopic methods in solution to provide valuable mechanistic insight.

Complex I is responsible for the catalytic reaction expressed by eq 1, where NADH is oxidized with ubiquinone (UQ) to



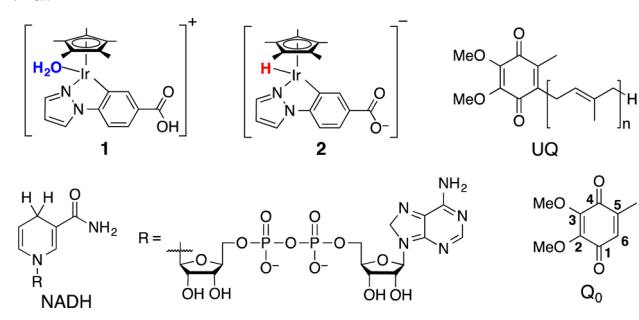
produce the corresponding oxidized form of NADH, that is, NAD^+ and the reduced form of UQ, that is, UQH_2 (ubiquinol).^{10,11} The transportation of two electrons from NADH to UQ is known to proceed via intervening Fe–S clusters and cytochromes with being associated with transportation of four protons from inside (H_{in}^+) to outside (H_{out}^+) across the membrane.^{12,13} Besides four protons transported through membrane, another one proton (H^+) would be consumed to form UQH_2 in the overall stoichiometric reaction in eq 1, indicating that the reaction represented by eq 1 might be acid-promoted as suggested by the electrochemical studies on the proton-coupled electron-transfer reduction of a ubiquinone coenzyme analogue.¹⁴ In this context, Complex I-dependent reduction of UQ has so far been examined in terms of the effect of the surrounding amino acid residues on the

Received: May 19, 2016

redox cofactors in various enzymatic aqueous reaction systems.¹⁵

However, in nonenzymatic reaction systems mimicking the function of Complex I, reduction of various substituted 1,4-benzoquinones as a model of UQ with NADH analogues has so far been investigated with regard to the proton-coupled electron transfer in both aqueous and organic solvents.^{16–18} However, there has so far been no report on the reaction between an NADH analogue and a UQ analogue bearing both dimethoxy and methyl substituents, since the strong electron-donating effect of these substituents has prohibited the reduction of UQ with NADH even under the acidic conditions. Furthermore, NADH is known to be unstable in an acidic medium at room temperature. Thus, the appropriate range of pH for the use of NADH is limited at pH > 7.¹⁹ The extremely low aqueous solubility of UQ as well as UQH₂ has also precluded further exploration of their redox reactivity in a homogeneous reaction system irrespective of the number ($n = 6–10$) of isoprenoid subunits in their side chain (Chart 1).

Chart 1. Ir Aqua Complex **1**, the Hydride Complex **2**, NADH, UQ, and 2,3-Dimethoxy-5-methyl-1,4-benzoquinone (Q₀)



Complex I by itself independent of other respiratory chain complexes is also responsible for the reduction of O₂ by NADH to form reactive oxygen species such as superoxide (O₂^{•-}) and hydrogen peroxide (H₂O₂) as an expression of NADH oxidase function of white blood cells.^{20,21} However, there has so far been no report on the reaction of O₂ with NADH catalyzed by a ubiquinone coenzyme analogue (UQ) to selectively form H₂O₂, although O₂ was selectively reduced by 1,4-hydroquinones via the autocatalytic production of H₂O₂ in nonenzymatic reaction system.²² H₂O₂ has merited increasing attention as an attractive clean energy and is expected to be utilized in H₂O₂ fuel cell.^{23–28}

We report herein the successful reduction of 2,3-dimethoxy-5-methyl-1,4-benzoquinone (Q₀) as a ubiquinone analogue with NADH to produce the corresponding ubiquinol (Q₀H₂) in water by using a water-soluble iridium aqua complex [Ir^{III}(Cp*)(4-(1H-pyrazol-1-yl-κN²)benzoic acid-κC³)(H₂O)]₂SO₄ [1]₂·SO₄, which can react with NADH to produce an Ir-hydride complex (**2**).²⁹ The coenzyme analogue Q₀ is soluble up to ~4.0 mM in water at pH 7 in contrast to water-insoluble ubiquinone coenzyme Q₁₀.³⁰ Moreover, the catalytic reduction of dioxygen by NADH was made possible to selectively generate hydrogen peroxide in the presence of [1]₂·SO₄ and a ubiquinone coenzyme analogue, Q₀.

EXPERIMENTAL SECTION

General Methods. All experiments were performed under an Ar or N₂ atmosphere by using standard Schlenk techniques unless

otherwise noted. UV–vis absorption spectra were recorded on a Hewlett–Packard 8453 diode array spectrophotometer with a quartz cuvette (light-path length = 1 cm) at 298 K. The mixed gas was controlled by using a gas mixer (Kofloc GB-3C, KOJIMA Instrument Inc.), which can mix two or more gases at a defined partial pressure and mass flow rate. A defined concentration of O₂ in an aqueous solution was prepared by a mixed gas flow of O₂ and N₂ controlled by using a gas flow meter (KOJIMA Instrument Inc.) appropriate for each gas under normal pressure (1.0 × 10⁻¹ MPa). The ¹H NMR spectra were recorded on JEOL JNM-AL300 spectrometer and Varian UNITY INOVA600. The pH values were determined by a pH meter (TOA, HM-20J) equipped with a pH combination electrode (TOA, GST-5725C). The pH of the solution was adjusted by using 1.00–10.0 M NaOH/H₂O without buffer unless otherwise noted.

Chemicals. Chemicals were purchased from commercial source and used without purification, unless otherwise noted. A water-soluble iridium complex **1** was synthesized and characterized as reported previously.^{29,31} An aqueous solution (50 mL) of [Ir^{III}(Cp*)(H₂O)₃](SO₄) (0.20 g, 0.423 mmol) and 4-(1H-pyrazol-1-yl)benzoic acid (0.085 g, 0.454 mmol) was stirred under reflux for 12 h. The reaction solution was filtered with a membrane filter (Toyo Roshi Kaisha, Ltd., H100A025A; pore diameter, 1 μm). The filtrate was evaporated under reduced pressure to yield a yellow powder of **1** and was dried in vacuo. 2,3-Dimethoxy-5-methyl-1,4-benzoquinone (>97.0%) was purchased from Wako Chemical, Ltd. 2,3-Dimethoxy-5-methylhydroquinone (>97.0%) was purchased from Astatech, Inc. β-Nicotinamide adenine dinucleotide disodium salt hydrate, reduced form, was purchased from Tokyo Chemical Industry Co., Ltd. Oxo[5,10,15,20-tetra(4-pyridyl)porphinato]titanium(IV) ([TiO(tpyp)]) was supplied from Tokyo Chemical Industry Co., Ltd. (TCI). H₂ (99.99%; Japan Air Gases Co.) and O₂ (99.5%; Sumitomo Seika Chemicals Co., Ltd.) gases were used without further purification. Purification of water (18.2 MΩ cm) was performed with a Milli-Q system (Millipore; Direct-Q 3 UV).

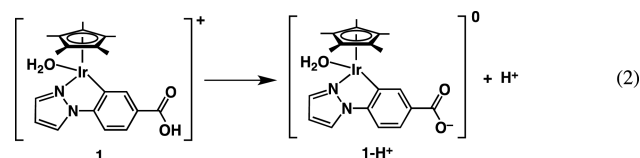
Detection of Hydrogen Peroxide. The amount of produced hydrogen peroxide was determined by spectroscopic titration with an acidic solution of [TiO(tpypH₄)]⁴⁺ complex (Ti-TPyP reagent).³² The Ti-TPyP reagent was prepared by dissolving 34.03 mg of the [TiO(tpyp)] complex in 1000 mL of 50 mM hydrochloric acid. A small portion (100 mL) of the reaction solution was sampled and diluted with water. To 0.25 mL of the diluted sample, 0.25 mL of 4.8 M perchloric acid and 0.25 mL of the Ti-TPyP reagent were added. The mixed solution was then allowed to stand for 5 min at room temperature. This sample solution was diluted to 2.5 mL with water and used for the spectroscopic measurement. The absorbance (A_S) at λ = 434 nm was measured by using a Hewlett–Packard 8453 diode array spectrophotometer. A blank solution was prepared in a similar manner by adding distilled water instead of the sample solution in the same volume with its absorbance designated as A_B. The difference in absorbance was determined as follows: ΔA₄₃₄ = A_B – A_S. On the basis of ΔA₄₃₄ and the volume of the solution, the amount of hydrogen peroxide was determined according to the literature.³²

pH Adjustment. The pH values of the solutions were determined by a pH meter (TOA, HM-20J) equipped with a pH combination electrode (TOA, GST-5725C). The pH of solution was adjusted by using 1.00–10.0 M NaOH/H₂O without buffer unless otherwise noted.

RESULTS AND DISCUSSION

The synthesis and characterization of **1** were performed according to the literature and are briefly described in the Experimental Section.^{29,31} The carboxylic acid group in **1** is deprotonated to give the carboxylate form **1-H⁺** as shown in eq 2 at pH > 7.0, since pK_a of **1** was determined to be 4.0 (eq 2).^{29,31}

The characteristic absorption band of the UV–vis absorption spectrum of NADH at λ_{max} = 260 and 340 nm and that of 2,3-dimethoxy-5-methyl-1,4-benzoquinone (Q₀) at λ_{max} = 269 nm gradually decreased, and finally the new absorption band at λ_{max}



= 260 nm assignable to NAD⁺ appeared in the presence of a catalytic amount of 1-H⁺ at pH 7.0, as shown in Figure 1.³³ In

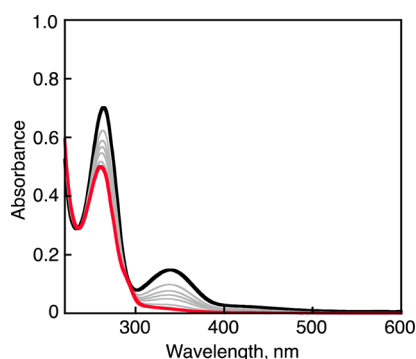


Figure 1. Changes in the UV-vis absorption spectra observed at $t = 0$ (black line) and 10 min (red line) in the reaction of Q_0 (25 μM) with NADH (25 μM) in the presence of **1** (2.5 μM) in an aqueous phosphate buffer (2.0 mL, pH 7.0) with stirring under argon at 298 K after addition of an aliquot of the solution of **1** (50 μL , 0.10 mM) injected by a syringe to the solution at $t = 0$.

contrast, there was no change in the UV-vis absorption spectra in the absence of **1** under otherwise the same experimental conditions (Figure S1 in Supporting Information). No formation of semiquinone radical anion ($\text{Q}_0^{\bullet-}$) at $\lambda_{\text{max}} = 320$ and 450 nm was confirmed throughout the reaction.³⁴ These results indicate that **1-H⁺** catalyzes the reduction of Q_0 with NADH to form 2,3-dimethoxy-5-methylhydroquinone (Q_0H_2) and NAD⁺ as expressed by eq 3 and Scheme 1.



The progress of the reaction was also monitored by ¹H NMR as shown in Figure 2. The disappearance of the peak at $\delta = 6.91$ ppm was due to the consumption of NADH, and the new peak appeared at $\delta = 2.08$ ppm that corresponds to a methyl group ($-\text{CH}_3$) of Q_0H_2 at 5 position indicating the stoichiometric

Scheme 1. Catalytic Cycle for the Reduction of Q_0 by NADH with **1**

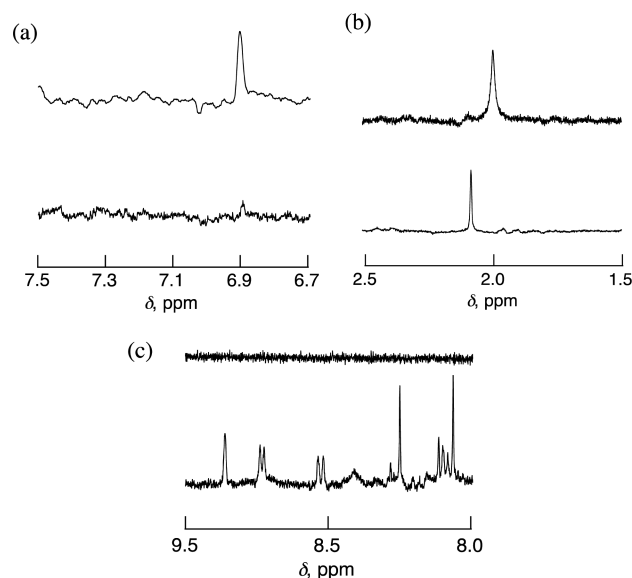
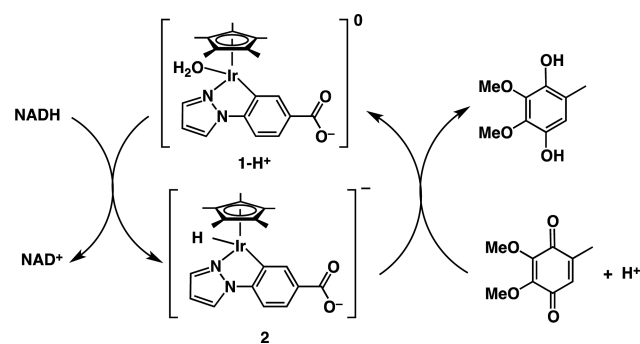
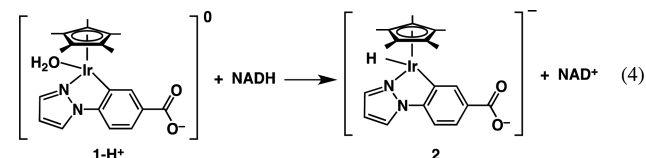


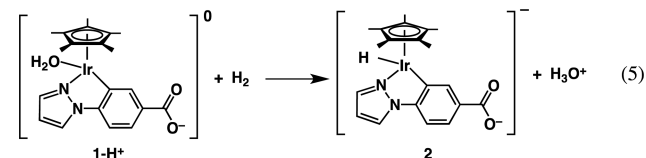
Figure 2. ¹H NMR spectra in the reaction of Q_0 (11.8 mM) with NADH (12.3 mM) catalyzed by **1** (0.10 mM) for 10 min in a deaerated aqueous phosphate buffer solution (pH 8.0) at 298 K. (a) ¹H NMR spectral of the authentic sample of NADH (12.3 mM) and reaction solution after 10 min; consumption of NADH. (b) The conversion from Q_0 ($\delta = 2.01$ ppm) to Q_0H_2 ($\delta = 2.08$ ppm). (c) The formation of NAD⁺ ($\delta \approx 8.0$ –9.5 ppm).

conversion from Q_0 to Q_0H_2 (Figure 2a,b).^{35,36} The simultaneous formation of NAD⁺ clearly yields the characteristic peaks at $\delta \approx 8.0$ –9.5 ppm in Figure 2c.^{29,37}

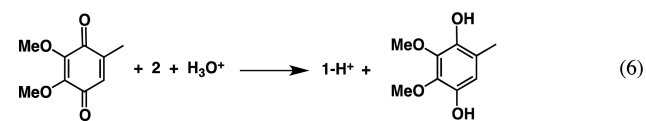
1-H⁺ was converted to the iridium(III) hydride complex **2** by the reduction with NADH in water at pH 8.8 as reported previously (eq 4).²⁹ The pK_a value of the protonated **2** may be



similar to that of **1** (4.0) because the pK_a value is similar to that of benzoic acid (4.19).³⁸ The formation of **2** was detected by ¹H NMR and electrospray ionization mass spectrometry.²⁹ The hydride complex **2** was also produced in the reaction of **1-H⁺** with hydrogen (H_2) as reported previously (eq 5).^{29,31}



The resulting **2** reduced Q_0 ($\lambda_{\text{max}} = 269$ and 412 nm) to produce 2,3-dimethoxy-5-methylhydroquinone (Q_0H_2 ; $\lambda_{\text{max}} = 285$ nm) in water (pH 7.0) at room temperature as expressed by eq 6 that was confirmed by UV-vis and ¹H NMR. Thus, Q_0



was catalytically reduced with H_2 to yield Q_0H_2 in the presence of 1-H^+ as shown by Figure 3. The characteristic absorption

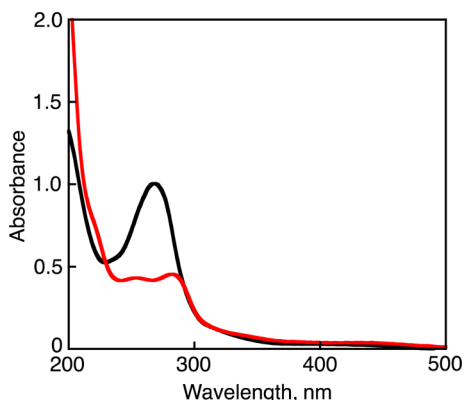
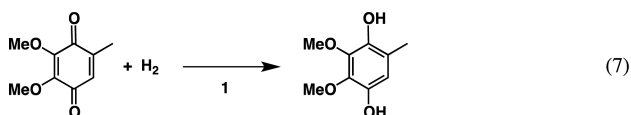
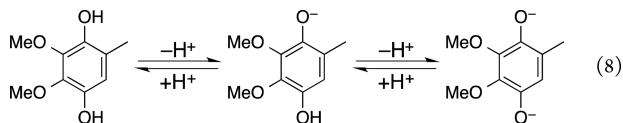


Figure 3. Changes in the UV-vis absorption spectrum during the reduction of Q_0 ($50 \mu\text{M}$) with H_2 (bubbling for 5 min) by using **1** ($25 \mu\text{M}$) in water (pH 7.0) at 298 K. An argon-saturated reaction solution of **1** and Q_0 (black line) was bubbled with H_2 (1.0×10^{-1} MPa) for 5 min thus resulting in the formation of Q_0H_2 (red line).

band due to Q_0 at $\lambda_{\text{max}} = 269$ nm gradually disappears, and the new absorption bands appear at $\lambda_{\text{max}} = 285$ and 254 nm assignable to QH_2 and **2**, respectively. The stoichiometry of the reaction is determined as given by eq 7 based on the extinction coefficients of Q_0 at $\lambda_{\text{max}} = 269$ nm ($\epsilon = 1.5 \times 10^4 \text{ M}^{-1} \text{ cm}^{-1}$) and Q_0H_2 at $\lambda_{\text{max}} = 285$ nm ($\epsilon = 4.1 \times 10^3 \text{ M}^{-1} \text{ cm}^{-1}$).³⁹

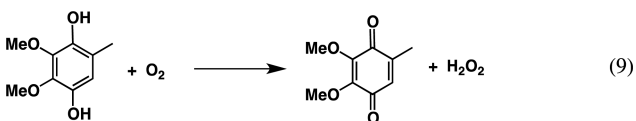


When the pH of a Q_0H_2 solution was increased from pH 7.0 to 10.8 by adding an aliquot of 0.1–5.0 M NaOH solution several times, a new absorption band at $\lambda_{\text{max}} = 307$ nm appeared with an isosbestic point at $\lambda = 289$ nm as shown in Figure 4a, indicating the formation of deprotonated anion (Q_0H^-) in eq 8. Further addition of NaOH to the solution resulted in the rise



of new absorption bands due to the corresponding dianion (Q_0^{2-} ; eq 8), that is, doubly deprotonated Q_0H_2 , with the shift of the absorption maxima from $\lambda_{\text{max}} = 307$ to 311 nm. From the UV-vis absorption spectral titration in Figure 4b, the pK_a values of Q_0H_2 were determined to be $\text{pK}_{a1} = 9.90$ and $\text{pK}_{a2} = 11.4$, respectively. These pK_a values are similar to those of hydroquinone.⁴⁰

Although Q_0H_2 is stable in neutral water under air for a few minutes, Q_0H_2 is gradually oxidized by O_2 (eq 9) in water at



various pH as observed by UV-vis absorption spectral change in Figure 5. The rate of the reaction to generate Q_0 and H_2O_2

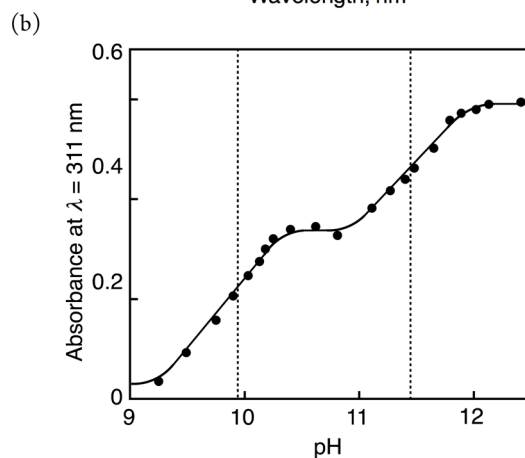
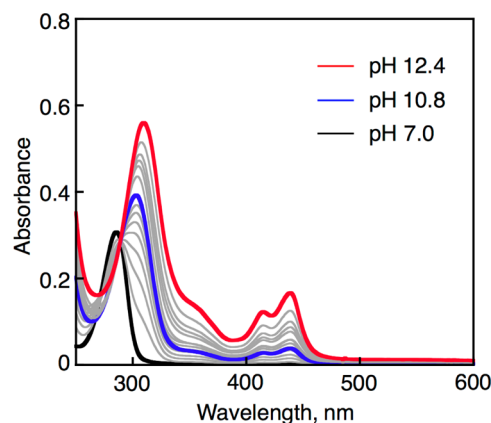


Figure 4. (a) UV-vis spectral changes of Q_0H_2 by the addition of NaOH in deaerated H_2O at pH 7.0 (black line), pH 10.8 (blue line), and pH 12.4 (red line) at 298 K. (b) Change in absorbance at $\lambda = 311$ nm by the addition of 0.10–5.0 M NaOH in deaerated H_2O at 298 K.

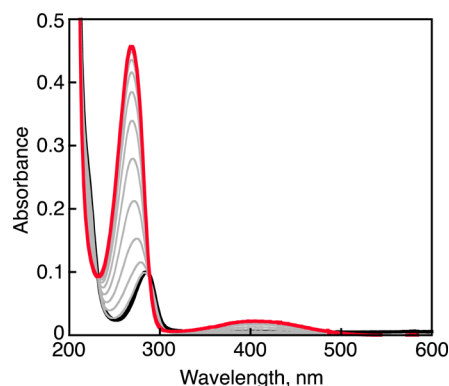


Figure 5. Changes in the UV-vis absorption spectra during the oxidation of Q_0H_2 ($30 \mu\text{M}$) by O_2 in an O_2 -saturated aqueous borate buffer solution (pH 8.0) at 298 K at $t = 0$ –10 min detected every 50 s. A $25 \mu\text{L}$ aliquot of a solution of Q_0H_2 (2.0 mM) was injected into 2.0 mL of an O_2 -saturated aqueous borate buffer solution (pH 8.0) at 298 K.

became much faster with increasing pH as observed in Figure 6 and Figure S2 in Supporting Information. With the progress of the reaction, the characteristic UV-vis absorption band of Q_0H_2 at $\lambda_{\text{max}} = 285$ nm changes gradually to that of Q_0 at $\lambda_{\text{max}} = 269$ nm, exhibiting the isosbestic points at $\lambda = 232$ and 289 nm (Figure 5). The amount of H_2O_2 produced in this reaction determined by the spectral titration with use of the oxo-[5,10,15,20-tetra(4-pyridyl)porphyrinato]titanium(IV) com-

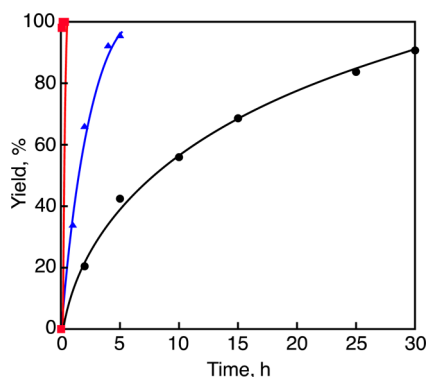


Figure 6. Time course of formation of Q_0 in the reaction of Q_0H_2 ($100 \mu M$) with O_2 (1.4 mM) in aqueous phosphate buffer at 298 K at various pH values (pH 6.0, 7.0, and 8.0; black ●, blue ▲, and red ■, respectively).

plex in water (see [Experimental Section](#))³² agrees well with that of Q_0H_2 consumed according to [eq 9](#) based on the extinction coefficients for Q_0H_2 ($\epsilon = 1.9 \times 10^3 \text{ M}^{-1} \text{ cm}^{-1}$) and Q_0 ($\epsilon = 1.5 \times 10^4 \text{ M}^{-1} \text{ cm}^{-1}$). A linear relationship between the concentrations of initial Q_0H_2 and resulting H_2O_2 was obtained with a slope of 1.0 as shown in [Figure 7](#). This indicates the validity of the stoichiometry of the reaction in [eq 9](#).

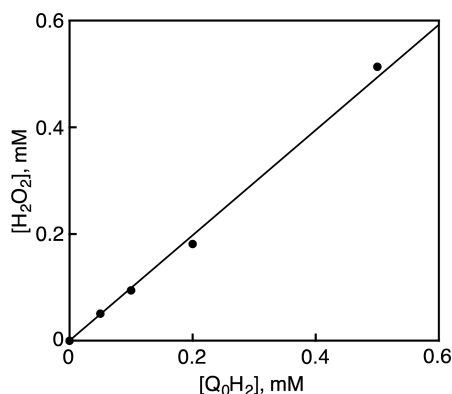
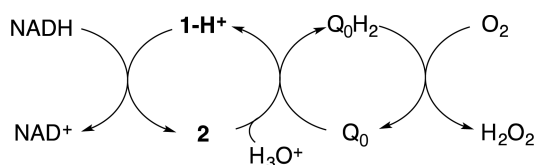


Figure 7. Plot of the concentration of H_2O_2 produced by the catalytic reduction of O_2 ($1.0 \times 10^{-1} \text{ MPa}$) with Q_0H_2 ($50 \mu M$ – 0.50 mM) at 298 K in an aqueous phosphate buffer solution (pH 8.0).

By combining [eqs 4, 6, and 9](#), the overall catalytic cycle for the selective H_2O_2 generation in the reaction of NADH with O_2 by using **1** and Q_0 as cocatalysts is shown in [Scheme 2](#), where $1-H^+$ reacts with NADH to produce the hydride **2**, which reduces Q_0 to Q_0H_2 followed by reduction of O_2 with Q_0H_2 to produce H_2O_2 , accompanied by regeneration of $1-H^+$ and Q_0 .

The generation of H_2O_2 in the reaction of NADH (0.20 mM) with O_2 (1.4 mM) in the presence of catalytic amount of **1** ($5.0 \mu M$) and Q_0 ($50 \mu M$) in an aqueous borate buffer

Scheme 2. Overall Catalytic Cycle for the Selective H_2O_2 Generation from NADH and O_2 with **1** and Q_0



solution at various pH (8.0, 9.0, and 10.4) is shown in [Figure 8](#). At pH 8.0, H_2O_2 was generated efficiently. When **1** ($1.0 \mu M$),

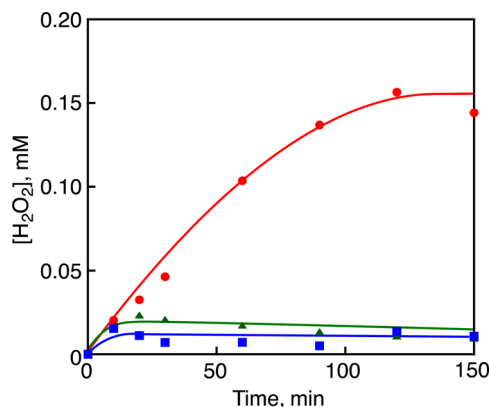
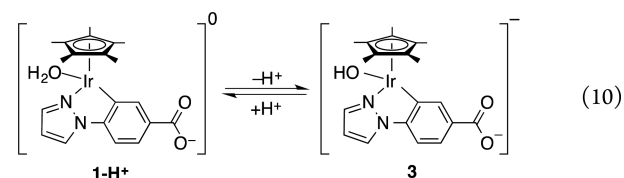


Figure 8. Time course of H_2O_2 production by the reaction of NADH (0.20 mM) with O_2 (1.4 mM) catalyzed by **1** ($5.0 \mu M$) and Q_0 ($50 \mu M$) in aqueous borate buffer at 298 K at various pH values (pH 8.0, 9.0, and 10.4; red ●, green ▲, and blue ■, respectively).

Q_0 ($50 \mu M$), and NADH (0.20 mM) were used, the turnover number (TON) of H_2O_2 production with respect to **1** reached 54 at 40 min. Under more basic conditions, $1-H^+$ complex released a proton from the aqua ligand to form the corresponding hydroxo complex **3**, leading to substitution inertness at the Ir metal center of the iridium complex **1**. The pK_a value was determined to be 9.5 ([eq 10](#)).²⁹ The reactivity of



Q_0H_2 for reduction of O_2 increased with increasing pH ([Figure 6](#)), whereas the iridium complex is deactivated by the deprotonation from the H_2O ligand ([eq 10](#)). In such a case pH 8.0 was found to be suitable for the catalytic H_2O_2 formation from NADH and O_2 by using **1** and Q_0 .

To determine the rate-determining step in the catalytic cycle, dependence of r on concentrations of substrates were examined in the catalytic generation of H_2O_2 from NADH and O_2 in the presence of **1** and Q_0 in an aqueous borate buffer (pH 8.0). When the concentrations of **1** and NADH were varied, the rates of H_2O_2 generation (r) were independent of the concentrations of **1** and NADH as shown in [Figures 9 and 10](#), respectively (the time courses are shown in [Figures S3 and S4](#) in [Supporting Information](#), respectively). These results indicate that **1** and NADH are not involved in the rate-determining step in the catalytic generation of H_2O_2 .

In contrast, when the concentrations of Q_0 and O_2 were varied, the rates of H_2O_2 generation (r) are proportional to concentrations of Q_0 and O_2 as shown in [Figures 11 and 12](#), respectively (the time courses are shown in [Figures S5 and S6](#) in [Supporting Information](#), respectively). Thus, the reaction rate is expressed by [eq 11](#), where

$$r = k[Q_0][O_2] \quad (11)$$

k is the second-order rate constant. The slope of the linear plot of r versus the concentration of Q_0 as shown in [Figure 11](#)

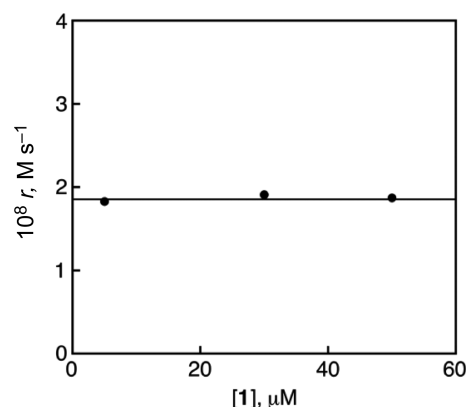


Figure 9. Plot of the initial rate of H_2O_2 production (r) vs concentration of **1** in the production of H_2O_2 from NADH (1.0 mM) and O_2 catalyzed by **1** (5.0, 30, and 50 μM) and Q_0 (50 μM) in an O_2 -saturated aqueous phosphate buffer (pH 8.0) at 298 K.

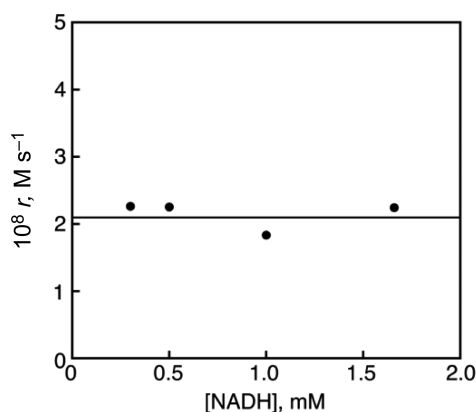


Figure 10. Plot of the initial rate of H_2O_2 production (r) vs concentration of NADH (0.30, 0.50, 1.00, and 1.66 mM) in the production of H_2O_2 from NADH and O_2 catalyzed by **1** (5.0 μM) and Q_0 (50 μM) in an O_2 -saturated aqueous phosphate buffer (pH 8.0) at 298 K.

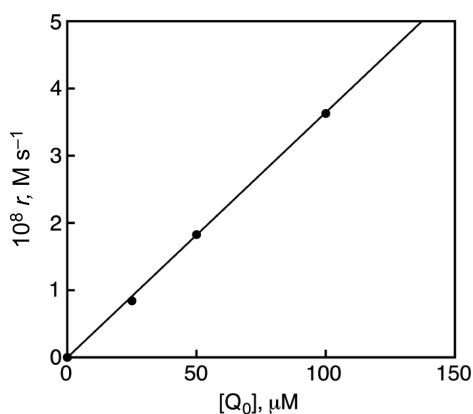


Figure 11. Plot of the initial rate of H_2O_2 production (r) vs concentration of Q_0 in the production of H_2O_2 from NADH (1.0 mM) and O_2 catalyzed by **1** (5.0 μM) and Q_0 (25, 50, and 100 μM) in an O_2 -saturated aqueous phosphate buffer (pH 8.0) at 298 K.

corresponds to $k[\text{O}_2]$ ($= k_{\text{obs}}$). On the one hand, from k_{obs} and fixed $[\text{O}_2]$, k was determined to be $0.28 \text{ M}^{-1} \text{ s}^{-1}$. On the other hand, the slope of the linear plot of r versus concentration of O_2 in Figure 12 corresponds to $k[\text{Q}_0]$ ($= k_{\text{obs}}$).

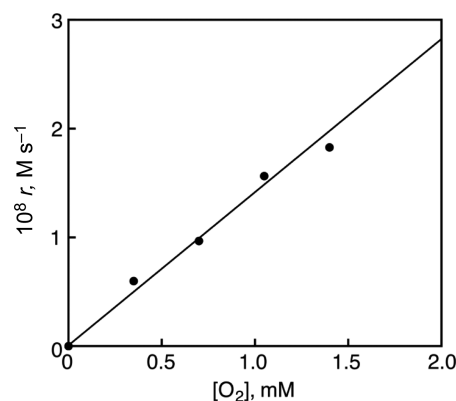


Figure 12. Plot of the initial rate of H_2O_2 production (r) vs concentration of O_2 (0.35, 0.70, 1.05, and 1.40 mM) in the production of H_2O_2 from NADH (1.0 mM) and O_2 catalyzed by **1** (5.0 μM) and Q_0 (50 μM) in an aqueous phosphate buffer (pH 8.0) at 298 K.

From k_{obs} and fixed $[\text{Q}_0]$, k was determined to be $0.28 \text{ M}^{-1} \text{ s}^{-1}$. These two second-order rate constants obtained from different plots agree well with each other, suggesting that the rate-determining step in the overall catalytic H_2O_2 production is the reduction of O_2 by Q_0H_2 . The rate constant of formation of **2** from 1-H^+ with NADH was reported to be $44 \text{ M}^{-1} \text{ s}^{-1}$ at 298 K,²⁹ which is much larger than the k value mentioned above. Thus, the reaction kinetics of oxidation of Q_0H_2 by O_2 (eq 9) was examined in the absence of NADH (vide infra).

The spectral change during the oxidation of Q_0H_2 by O_2 was shown in Figure 5. The time course of the reaction was monitored by the increase in absorbance at $\lambda = 269 \text{ nm}$ due to Q_0 as shown in Figure 13, which exhibits a sigmoidal curve with

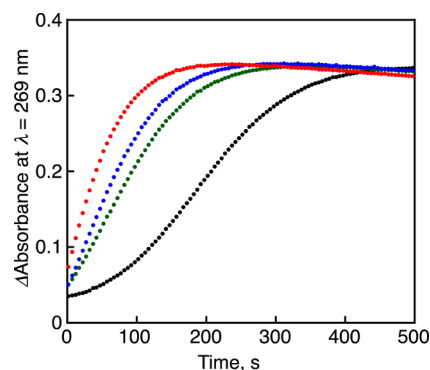


Figure 13. Time course of change in absorbance at $\lambda = 269 \text{ nm}$ for the formation of Q_0 in the reduction of O_2 (1.4 mM) with Q_0H_2 (25 μM) in the absence and presence of a catalytic and stoichiometric amount of Q_0 (0, 5.0, 10, and 25 μM ; black, green, blue, and red, respectively) in an aqueous borate buffer solution (pH 8.0) at 298 K. In this figure, the amount of Q that is added into the solution was withheld.

an induction period. Interestingly, when a catalytic and stoichiometric amount of the product (Q_0) was added to a reaction solution, the induction period disappeared, and the rate of formation of Q_0 was accelerated with increasing concentration of Q_0 (Figure 13 and Figure S7 in Supporting Information). These results indicate that the oxidation of Q_0H_2 by O_2 proceeds in an autocatalytic fashion. In addition, there was no difference in the induction period when a stoichiometric amount of 1-H^+ was added to this reaction solution (Figure 14 and Figure S8 in Supporting Information), indicating that the

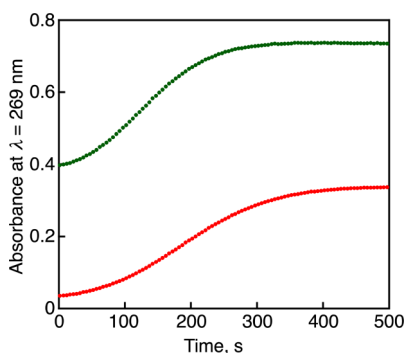
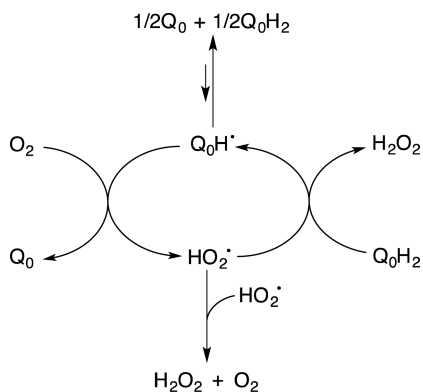


Figure 14. Time course of change in absorbance at $\lambda = 269$ nm for the formation of Q_0 in the reduction of O_2 (1.4 mM) with Q_0H_2 (25 μ M) in the absence and presence of a stoichiometric amount of $1-H^+$ (0 and 25 μ M; red and green, respectively) in an aqueous borate buffer solution (pH 8.0) at 298 K.

iridium complex has nothing to do with the oxidation of Q_0H_2 by O_2 . In addition, the rate of formation of H_2O_2 by the reduction of O_2 (1.4 mM) by Q_0H_2 (25 μ M), which is calculated to be $1.0 \times 10^{-8} \text{ M s}^{-1}$ using the k value ($0.28 \text{ M}^{-1} \text{ s}^{-1}$), agrees with the initial rate without Q_0 in Figure 13 ($1.2 \times 10^{-8} \text{ M s}^{-1}$).

The autocatalytic cycle for the oxidation of Q_0H_2 by O_2 may proceed as shown in Scheme 3, where Q_0H^\bullet is formed in the

Scheme 3. Autocatalytic Radical Chain Reactions for Oxidation of Q_0H_2 by O_2



comproportionation reaction of Q_0 and Q_0H_2 . Q_0H^\bullet reacts with O_2 to produce HO_2^\bullet accompanied by regeneration of Q_0 .⁴¹ HO_2^\bullet reacts with Q_0H_2 to produce H_2O_2 , accompanied by regeneration of Q_0H^\bullet . Acceleration of the rate with increasing concentration of the product (Q_0) in Figure 13 can be rationalized by the autocatalytic cycle in Scheme 3, where Q_0 is involved in the initiation step. The hydrogen abstraction reaction of HO_2^\bullet from Q_0H_2 may be the rate-determining step, because the rate of formation of Q_0 at the steady state was proportional to $[Q_0H_2]^{3/2}$ (Figure S9 and see the steady-state kinetic analysis). The overall catalytic O_2 reduction by NADH with iridium complex $1-H^+$ and Q_0 as catalysts proceeds via rate-determining autocatalytic chain reaction, where O_2 is reduced by Q_0H_2 . Judging from the time course of the catalytic reduction of Q_0 by NADH with **1** in Figure 1, this is not the rate-determining step as compared with the catalytic reduction of O_2 by NADH with **1** and Q_0 .

CONCLUSION

In conclusion, a water-soluble iridium(III) complex **1** catalyzes the reduction of coenzyme Q_0 as a ubiquinone analogue by NADH in water at room temperature via the reduction of **1** by NADH to produce the hydride complex **2**, which reduces Q_0 to QH_2 , acting as a functional mimic of respiratory chain complex I. O_2 was reduced by Q_0H_2 via an autocatalytic pathway to generate the stoichiometric amount of H_2O_2 . Thus, the overall catalytic reduction of dioxygen by NADH proceeds to generate hydrogen peroxide in the presence of **1** and a ubiquinone coenzyme analogue, Q_0 , acting as cocatalysts (Scheme 2). Because NADH is regenerated by the reduction of NAD^+ by H_2 with $1-H^+$,²⁹ H_2O_2 can be produced by the reduction of O_2 by H_2 using $1-H^+$ as an inorganic catalyst instead of an industrial anthraquinone method for the production of H_2O_2 by H_2 .

ASSOCIATED CONTENT

Supporting Information

The Supporting Information is available free of charge on the ACS Publications website at DOI: 10.1021/acs.inorgchem.6b01220.

UV-vis absorption spectra, plot of H_2O_2 concentration versus time as O_2 is reduced by NADH in presence of Q_0 catalyzed by **1**, discussion of derived equations (PDF)

AUTHOR INFORMATION

Corresponding Authors

*E-mail: fukuzumi@chem.eng.osaka-u.ac.jp. (S.F.)

*E-mail: suenobu@chem.eng.osaka-u.ac.jp. (T.S.)

Notes

The authors declare no competing financial interest.

ACKNOWLEDGMENTS

This work was supported by ALCA and SENTAN projects from JST (to S.F.) and JSPS KAKENHI (Grant No. 16H02268 to S.F. and No. 16K05721 to T.S.), Japan.

REFERENCES

- (1) (a) Lin, B.-Y.; Kao, M.-C. *Ann. N. Y. Acad. Sci.* **2015**, *1350*, 17–28. (b) Babot, M.; Birch, A.; Labarbuta, P.; Galkin, A. *Biochim. Biophys. Acta, Bioenerg.* **2014**, *1837*, 1083–1092. (c) Hirst, J. *Annu. Rev. Biochem.* **2013**, *82*, 551–575. (d) Efremov, R. G.; Sazanov, L. A. *Curr. Opin. Struct. Biol.* **2011**, *21*, 532–540.
- (2) (a) Walker, J. E. *Q. Rev. Biophys.* **1992**, *25*, 253–324. (b) Yagi, T.; Matsuno-Yagi, A. *Biochemistry* **2003**, *42*, 2266–2274. (c) Ohnishi, T. *Biochim. Biophys. Acta, Bioenerg.* **1998**, *1364*, 186–206. (d) Sazanov, L. A. *Biochemistry* **2007**, *46*, 2275–2288. (e) Hirst, J. *Biochem. J.* **2010**, *425*, 327–339. (f) Verkhovskaya, M. L.; Belevich, N.; Euro, L.; Wikström, M.; Verkhovskiy, M. I. *Proc. Natl. Acad. Sci. U. S. A.* **2008**, *105*, 3763–3767.
- (3) (a) Lenaz, G.; Tioli, G.; Falasca, A. I.; Genova, M. L. *Biochim. Biophys. Acta, Bioenerg.* **2016**, *1857*, 991–1000. (b) Davoudi, M.; Kotarsky, H.; Hansson, E.; Fellman, V. *PLoS One* **2014**, *9*, e86767. (c) Lapuente-Brun, E.; Moreno-Loshuertos, R.; Acín-Pérez, R.; Latorre-Pellicer, A.; Colás, C.; Balsa, E.; Perales-Clemente, E.; Quirós, P. M.; Calvo, E.; Rodríguez-Hernández, M. A.; Navas, P. C.; Cruz, R.; Carracedo, Á.; López-Otín, C.; Pérez-Martos, A.; Fernández-Silva, P.; Fernández-Vizcarra, E.; Enriquez, J. A. *Science* **2013**, *340*, 1567–1570. (d) Dudkina, N. V.; Kudryashev, M.; Stahlberg, H.; Boekema, E. J. *Proc. Natl. Acad. Sci. U. S. A.* **2011**, *108*, 15196–15200. (e) Dudkina, N. V.; Eubel, H.; Keegstra, W.; Boekema, E. J.; Braun, H.-P. *Proc. Natl. Acad. Sci. U. S. A.* **2005**, *102*, 3225–3229. (f) Schäfer, E.; Dencher, N. A.; Vonck, J.; Parcej, D. N. *Biochemistry* **2007**, *46*,

- 12579–12585. (g) Zickermann, V.; Wirth, C.; Nasiri, H.; Siegmund, K.; Schwalbe, H.; Hunte, C.; Brandt, U. *Science* **2015**, *347*, 44–49.
- (4) Yankovskaya, V.; Horsefield, R.; Törnroth, S.; Luna-Chavez, C. S.; Miyoshi, H.; Léger, C.; Byrne, B.; Cecchini, G.; Iwata, S. *Science* **2003**, *299*, 700–704.
- (5) Sun, F.; Huo, X.; Zhai, Y.; Wang, A.; Xu, J.; Su, D.; Bartlam, M.; Rao, Z. *Cell* **2005**, *121*, 1043–1057.
- (6) (a) Genova, M. L. *Adv. Photosynth. Respir.* **2014**, *39*, 401–417. (b) Lenaz, G.; Genova, M. L. *Biochim. Biophys. Acta, Bioenerg.* **2009**, *1787*, 563–573.
- (7) Aberg, F.; Appelkvist, E. L.; Dallner, G.; Ernster, L. *Arch. Biochem. Biophys.* **1992**, *295*, 230–234.
- (8) (a) Yang, X.; Zhang, Y.; Xu, H.; Luo, X.; Yu, J.; Liu, J.; Chang, R. *Curr. Top. Med. Chem.* **2015**, *16*, 858–866. (b) Beal, M. F. *J. Bioenerg. Biomembr.* **2004**, *36*, 381–386.
- (9) (a) Schultz, J. R.; Ellerby, L. M.; Gralla, E. B.; Valentine, J. S.; Clarke, C. F. *Biochemistry* **1996**, *35*, 6595–6603. (b) Roginsky, V.; Barsukova, T. *J. Chem. Soc., Perkin Trans. 2* **2000**, 1575–1582.
- (10) Wikström, M.; Hummer, G. *Proc. Natl. Acad. Sci. U. S. A.* **2012**, *109*, 4431–4436.
- (11) (a) Friedrich, T.; Dekovic, D. K.; Burschel, S. *Biochim. Biophys. Acta, Bioenerg.* **2016**, *1857*, 214–223. (b) Ripple, M. O.; Kim, N.; Springett, R. *J. Biol. Chem.* **2013**, *288*, 5374–5380.
- (12) (a) Hirst, J.; Roessler, M. M. *Biochim. Biophys. Acta, Bioenerg.* **2016**, *1857*, 872–883. (b) Brandt, U. *Annu. Rev. Biochem.* **2006**, *75*, 69–92.
- (13) Baradaran, R.; Berrisford, J.-M.; Minhas, G. S.; Sazanov, L. A. *Nature* **2013**, *494*, 443–448.
- (14) (a) Lemmer, C.; Bouvet, M.; Meunier-Prest, R. *Phys. Chem. Chem. Phys.* **2011**, *13*, 13327–13332. (b) Greaves, M. D.; Niemz, A.; Rotello, V. M. *J. Am. Chem. Soc.* **1999**, *121*, 266–267. (c) Bauscher, M.; Mäntele, W. *J. Phys. Chem.* **1992**, *96*, 11101–11108. (e) Yuasa, J.; Yamada, S.; Fukuzumi, S. *Chem. - Eur. J.* **2008**, *14*, 1866–1874.
- (15) (a) Xia, L.; Björnstedt, M.; Nordman, T.; Eriksson, L. C.; Olsson, J. M. *Eur. J. Biochem.* **2001**, *268*, 1486–1490. (b) Verkhnovskaya, M.; Wikström, M. *Biochim. Biophys. Acta, Bioenerg.* **2014**, *1837*, 246–250. (c) Takahashi, T.; Yamaguchi, T.; Shitashige, M.; Okamoto, T.; Kishi, T. *Biochem. J.* **1995**, *309*, 883–890. (d) Stocker, R.; Suarna, C. *Biochim. Biophys. Acta, Gen. Subj.* **1993**, *1158*, 15–22. (e) Rauchová, H.; Fato, R.; Drahota, Z.; Lenaz, G. *Arch. Biochem. Biophys.* **1997**, *344*, 235–241.
- (16) (a) Anne, A.; Moiroux, J.; Savéant, J. M. *J. Am. Chem. Soc.* **1993**, *115*, 10224–10230. (b) Cheng, J. P.; Lu, Y.; Zhu, X. Q.; Mu, L. J. *J. Org. Chem.* **1998**, *63*, 6108–6114. (c) Miller, L. L.; Valentine, J. R. *J. Am. Chem. Soc.* **1988**, *110*, 3982–3989.
- (17) (a) Liu, Z.; Sadler, P. J. *Acc. Chem. Res.* **2014**, *47*, 1174–1185. (b) Liu, Z.; Deeth, R. J.; Butler, J. S.; Habtemariam, A.; Newton, M. E.; Sadler, P. J. *Angew. Chem., Int. Ed.* **2013**, *52*, 4194–4197. (c) Betanzos-Lara, S.; Liu, Z.; Habtemariam, A.; Pizarro, A. M.; Qamar, B.; Sadler, P. J. *Angew. Chem., Int. Ed.* **2012**, *51*, 3897–3900.
- (18) (a) Fukuzumi, S.; Fujii, Y.; Suenobu, T. *J. Am. Chem. Soc.* **2001**, *123*, 10191–10199. (b) Fukuzumi, S.; Kotani, H.; Lee, Y. M.; Nam, W. *J. Am. Chem. Soc.* **2008**, *130*, 15134–15142. (c) Yuasa, J.; Yamada, S.; Fukuzumi, S. *J. Am. Chem. Soc.* **2008**, *130*, 5808–5820. (d) Yuasa, J.; Yamada, S.; Fukuzumi, S. *Angew. Chem., Int. Ed.* **2008**, *47*, 1068–1071. (e) Fukuzumi, S.; Ohkubo, K.; Tokuda, Y.; Suenobu, T. *J. Am. Chem. Soc.* **2000**, *122*, 4286–4294. (f) Ishikawa, M.; Fukuzumi, S. *J. Chem. Soc., Faraday Trans.* **1990**, *86*, 3531–3536. (g) Fukuzumi, S.; Ishikawa, M.; Tanaka, T. *J. Chem. Soc., Perkin Trans. 2* **1989**, 1811–1816. (h) Fukuzumi, S.; Koumitsu, S.; Hironaka, K.; Tanaka, T. *J. Am. Chem. Soc.* **1987**, *109*, 305–316. (i) Fukuzumi, S.; Ishikawa, M.; Tanaka, T. *Tetrahedron* **1986**, *42*, 1021–1034. (j) Fukuzumi, S.; Nishizawa, N.; Tanaka, T. *J. Org. Chem.* **1984**, *49*, 3571–3578.
- (19) (a) Rover, L., Jr.; Fernandes, J. C. B.; de Oliveria Neto, G.; Kubota, L. T.; Katekawa, E.; Serrano, S. H. P. *Anal. Biochem.* **1998**, *260*, 50–55. (b) Markham, K. A.; Sikorski, R. S.; Kohen, A. *Anal. Biochem.* **2003**, *322*, 26–32. (c) Wu, J. T.; Wu, L. H.; Knight, J. A. *Clin. Chem.* **1986**, *32*, 314–319.
- (20) (a) Murphy, M. P. *Biochem. J.* **2009**, *417*, 1–13. (b) Seifert, E. L.; Estey, C.; Xuan, J. Y.; Harper, M.-E. *J. Biol. Chem.* **2010**, *285*, 5748–5758. (c) Kushnareva, Y.; Murphy, A. N.; Andreyev, A. Y. *Biochem. J.* **2002**, *368*, 545–553. (d) Liu, Y.; Fiskum, G.; Schubert, D. *J. Neurochem.* **2002**, *80*, 780–787.
- (21) Treberg, J. R.; Quinlan, C. L.; Brand, M. D. *J. Biol. Chem.* **2011**, *286*, 27103–27110.
- (22) (a) Sella, E.; Shabat, D. *Org. Biomol. Chem.* **2013**, *11*, 5074–5078. (b) Hiramoto, K.; Mochizuki, R.; Kikugawa, K. *J. Oleo Sci.* **2001**, *50*, 21–28.
- (23) (a) Fukuzumi, S.; Yamada, Y.; Karlin, K. D. *Electrochim. Acta* **2012**, *82*, 493–511. (b) Fukuzumi, S.; Yamada, Y. *Aust. J. Chem.* **2014**, *67*, 354–364. (c) Fukuzumi, S. *Biochim. Biophys. Acta, Bioenerg.* **2016**, *1857*, 604–611.
- (24) (a) Sanli, A. E. *Int. J. Energy Res.* **2013**, *37*, 1488–1497. (b) Disselkamp, R. S. *Energy Fuels* **2008**, *22*, 2771–2774.
- (25) (a) Yamada, Y.; Yoneda, M.; Fukuzumi, S. *Inorg. Chem.* **2014**, *53*, 1272–1274. (b) Yamada, Y.; Yoshida, S.; Honda, T.; Fukuzumi, S. *Energy Environ. Sci.* **2011**, *4*, 2822–2825. (c) Yamada, Y.; Yoneda, M.; Fukuzumi, S. *Chem. - Eur. J.* **2013**, *19*, 11733–11741.
- (26) (a) Yang, F.; Cheng, K.; Xiao, X.; Yin, J.; Wang, G.; Cao, D. *J. Power Sources* **2014**, *245*, 89–94. (b) Yang, F.; Cheng, K.; Wu, T.; Zhang, Y.; Yin, J.; Wang, G.; Cao, D. *Electrochim. Acta* **2013**, *99*, 54–61. (c) Yang, F.; Cheng, K.; Wu, T.; Zhang, Y.; Yin, J.; Wang, G.; Cao, D. *RSC Adv.* **2013**, *3*, 5483–5490.
- (27) Kato, S.; Jung, J.; Suenobu, T.; Fukuzumi, S. *Energy Environ. Sci.* **2013**, *6*, 3756–3764.
- (28) Yamada, Y.; Yoneda, M.; Fukuzumi, S. *Energy Environ. Sci.* **2015**, *8*, 1698–1701.
- (29) Maenaka, Y.; Suenobu, T.; Fukuzumi, S. *J. Am. Chem. Soc.* **2012**, *134*, 367–374.
- (30) (a) Siekmann, B.; Westesen, K. *Pharm. Res.* **1995**, *12*, 201–208. (b) Gu, J.; Chi, S.-M.; Zhao, Y.; Zheng, P.; Ruan, Q.; Zhao, Y.; Zhu, H.-Y. *Helv. Chim. Acta* **2011**, *94*, 1608–1617. (c) Kagan, V. E.; Arroyo, A.; Tyurin, V. A.; Tyurina, Y. Y.; Villalba, J. M.; Navas, P. *FEBS Lett.* **1998**, *428*, 43–46.
- (31) Maenaka, Y.; Suenobu, T.; Fukuzumi, S. *Energy Environ. Sci.* **2012**, *5*, 7360–7367. (b) Maenaka, Y.; Suenobu, T.; Fukuzumi, S. *J. Am. Chem. Soc.* **2012**, *134*, 9417–9427. (c) Shibata, S.; Suenobu, T.; Fukuzumi, S. *Angew. Chem., Int. Ed.* **2013**, *52*, 12327–12331.
- (32) Matsubara, C.; Kawamoto, N.; Takamura, K. *Analyst* **1992**, *117*, 1781–1784.
- (33) Hikosaka, K.; Kim, J.; Kajita, M.; Kanayama, A.; Miyamoto, Y. *Colloids Surf., B* **2008**, *66*, 195–200.
- (34) Görner, H. *Photochem. Photobiol.* **2003**, *78*, 440–448.
- (35) Wilczynski, J. J.; Daves, G. D., Jr.; Folkers, K. *J. Am. Chem. Soc.* **1968**, *90*, 5593–5598.
- (36) Yu, X.-J.; Chen, F.-E.; Dai, H.-F.; Chen, X.-X.; Kuang, Y.-Y.; Xie, B. *Helv. Chim. Acta* **2005**, *88*, 2575–2581.
- (37) Yan, Y. K.; Melchart, M.; Habtemariam, A.; Peacock, A. F. A.; Sadler, P. J. *JBIC, J. Biol. Inorg. Chem.* **2006**, *11*, 483–488.
- (38) Rived, F.; Rosés, M.; Bosch, E. *Anal. Chim. Acta* **1998**, *374*, 309–324.
- (39) Li, W.-W.; Hellwig, P.; Ritter, M.; Haehnel, W. *Chem. - Eur. J.* **2006**, *12*, 7236–7245.
- (40) (a) Quan, M.; Sanchez, D.; Wasylkiw, M. F.; Smith, D. K. *J. Am. Chem. Soc.* **2007**, *129*, 12847–12856. (b) Babaei, A.; McQuillan, A. J. *J. Electroanal. Chem.* **1998**, *441*, 197–203. (c) Bishop, C. A.; Tong, L. K. *J. Am. Chem. Soc.* **1965**, *87*, 501–505. (d) Baxendale, J. H.; Hardy, H. R. *Trans. Faraday Soc.* **1953**, *49*, 1140–1144.
- (41) For other examples of autocatalytic radical chain reactions, see: (a) Nishida, Y.; Lee, Y.-M.; Nam, W.; Fukuzumi, S. *J. Am. Chem. Soc.* **2014**, *136*, 8042–8049. (b) Morimoto, Y.; Lee, Y.-M.; Nam, W.; Fukuzumi, S. *Chem. Commun.* **2013**, *49*, 2500–2502. (c) Comba, P.; Lee, Y.-M.; Nam, W.; Waleska, A. *Chem. Commun.* **2014**, *50*, 412–414. (d) Bakač, A. *Inorg. Chem.* **1998**, *37*, 3548–3552.